IN-HAND MANIPULATION: GEOMETRY AND ALGORITHMS

Attawith Sudsang and Jean Ponce
Beckman Institute, University of Illinois, Urbana, IL 61801

Abstract: This paper addresses the problem of manipulating three-dimensional objects with a reconfigurable gripper. A detailed analysis of the problem geometry in configuration space is used to devise a simple and efficient algorithm for manipulation planning. The proposed approach has been implemented and preliminary simulation experiments are discussed.

1 Introduction

We address the problem of manipulating three-dimensional polyhedral objects using a new reconfigurable gripper, currently under construction at the University of Illinois [12]. The gripper consists of two parallel plates whose distance can be adjusted by a computer-controlled actuator (Figure 1). The bottom plate is a bare plane, and the top plate carries a rectangular grid of actuated pins that can translate in discrete increments under computer control. The details of the gripper design can be found in [12], where a grasp planning algorithm based on Rimon's and Burdick's notion of second-order immobility [11] is also presented.

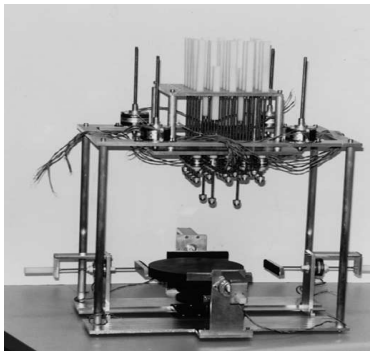

Figure 1. The prototype of a reconfigurable gripper.

We propose here an efficient algorithm for manipulating an object within a grasp by planning the sequence of pin configurations that will bring this object to a desired position and orientation. It is based on a detailed analysis of the geometry of the joint object/gripper configuration space. Characterizing the range of possible object motions associated with a grasp configuration allows us to identify the "minimal" configurations for which the object is totally immobilized as well as the "maximal" ones for which there is a non-empty open set of object motions within the grasp, but no escape path to infinity.

More precisely, our approach is based on the concept of *inescapable configuration space* (ICS) region, i.e., on the idea of characterizing the regions of configuration space for which the object is not immobilized but is constrained to lie within a bounded region of the free configuration space (see [10] for related work in the two-dimensional, two-finger case). ICS regions will allow us to plan in-hand object motions as sequences of gripper configurations (see [1, 4, 5, 6, 7, 9, 10] for related work): starting from some immobilizing configuration, we can open the gripper jaws and retract the immobilizing pins, then choose another triple of pins whose ICS region contains the initial gripper configuration, lower these pins, and as the jaws close, move the object to the corresponding immobilized configuration. Note that this approach does not require modeling what happens when contact occurs, but it requires frictionless contacts to avoid wedging. As explained in [12], the gripper is designed to minimize the amount of friction at the contacts.

2 Geometry of the Problem

The gripper shown in Figure 1 can be used to hold a polyhedral object through contacts with three of the top plate pins, and either a face, an edge-and-vertex, or a three-vertex contact with the bottom plate. We will assume throughout the paper that the faces of the polyhedron are triangular and detail the analysis of a face contact between the object and the bottom plate. It should be noted that this is for the sake of simplicity and conciseness only: arbitrary convex faces and other types of contacts can be handled as well.

Let us consider a contact between the bottom plate and a triangular face f with inward unit normal $\boldsymbol{n}$ and vertices $\boldsymbol{v}_i$ $(i = 1, 2, 3)$ and denote by f_i $(i = 1, 2, 3)$ the remaining faces, with inward unit normals $\boldsymbol{n}_i$ (Figure 2).

We assume without loss of generality that the four

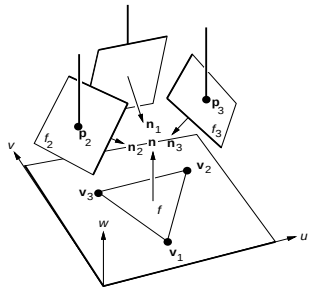

Figure 2. The four faces involved in a grasp.

vectors $\boldsymbol{n}$ and $\boldsymbol{n}_i$ $(i = 1, 2, 3)$ *positively span* $\mathbb{R}^3$, i.e., that a strictly positive linear combination of these vectors is equal to zero (this is a necessary condition for essential equilibrium). Given the physical layout of our gripper, contact between the upper-jaw pins and faces such that $\boldsymbol{n} \cdot \boldsymbol{n}_i > 0$ is of course impossible, and we further assume without loss of generality that $\boldsymbol{n} \cdot \boldsymbol{n}_i < 0$ for $i = 1, 2, 3$.

Under these assumptions, we can choose a coordinate system (u, v, w) attached to the object with w axis parallel to $\boldsymbol{n}$, and write in this coordinate system $\boldsymbol{n} = (0, 0, 1)^T$ and $\boldsymbol{n}_i = \frac{1}{l_i}(a_i, b_i, -1)^T$, where $l_i = \sqrt{1 + a_i^2 + b_i^2}$.

Likewise, since the vectors $\boldsymbol{n}$ and $\boldsymbol{n}_i$ $(i = 1, 2, 3)$ positively span $\mathbb{R}^3$, we can write $\boldsymbol{n} = -\sum_{i=1}^{3} \mu_i \boldsymbol{n}_i$, where $\mu_i > 0$ for $i = 1, 2, 3$. To complete the specification of the faces f_i $(i = 1, 2, 3)$, we will denote by c_i the height of f_i at the origin, so the plane of this face can be parameterized by $w_i = a_i u_i + b_i v_i + c_i$. Finally, since the faces f_i are triangular, we will express the fact that the point associated with the parameters u_i, v_i actually belongs to f_i by linear inequalities on u_i, v_i:

$$a_{ij} u_i + b_{ij} v_i + c_{ij} \leq 0, \quad j = 1, 2, 3. \tag{1}$$

2.1 Contact

We reduce the problem of achieving contact between a spherical pin and a plane to the problem of achieving point contact with a plane. This is done without loss of generality by growing the object to be fixtured by the pin radius and shrinking the spherical end of the pin into its center (see [2, 13, 14] for a similar approach in the two-dimensional case). We attach a coordinate system (q, r, w) to the gripper, and denote by $\mathcal{R}$ and $\boldsymbol{t}$ the rotation of angle θ about $\boldsymbol{n}$ and the translation (x, y) in the plane orthogonal to $\boldsymbol{n}$ that map the (q, r, w) coordinate system onto the (u, v, w) coordinate system.

If $\boldsymbol{p}_i$ and $\boldsymbol{q}_i$ denote respectively the positions of the tip of pin number i in the object's and gripper's coordinate frames, we can write $\boldsymbol{p}_i = (u_i, v_i, a_i u_i + b_i v_i + c_i)$, $\boldsymbol{q}_i = (q_i, r_i, \delta - h_i)^T$ and

$$\boldsymbol{q}_i = \mathcal{R} \boldsymbol{p}_i + \boldsymbol{t}, \tag{2}$$

where q_i, r_i and h_i denote respectively the integer pin position on the bottom plate grid and its height, and δ is the jaw separation.

Equation (2) is a condition for contact between pin number i and the corresponding face. It can be rewritten as $\mathcal{C}_i(x, y, \theta, \delta) = 0$, where

$$\begin{aligned} \mathcal{C}_i(x, y, \theta, \delta) \stackrel{\text{def}}{=} & (x - q_i)\cos(\theta + \alpha_i) \\ & + (y - r_i)\sin(\theta + \alpha_i) + d_i \delta - e_i, \end{aligned}$$

$\alpha_i = \text{Arg}(a_i, b_i)$, $d_i = 1/\sqrt{a_i^2 + b_i^2}$, and $e_i = d_i(c_i + h_i)$.[1] Note that α_i is simply the angle between the u axis and the projection of $\boldsymbol{n}_i$ onto the u, v plane (Figure 3).

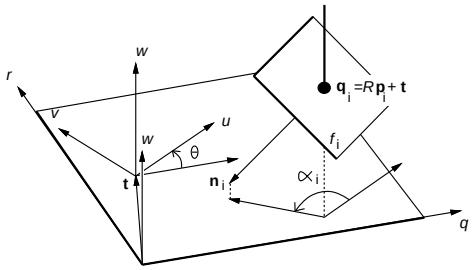

Figure 3. Contact between a pin and a face.

The three pins will be in contact with the corresponding faces when $\mathcal{C}_i(x, y, \theta, \delta) = 0$ is satisfied for $i = 1, 2, 3$. In particular, any linear combination $\sum_{i=1}^{3} \xi_i \mathcal{C}_i(x, y, \theta, \delta)$ of the contact constraints will also be equal to zero. In particular, if we choose $\xi_i = \mu_i / (d_i l_i)$, we can use the relation $\boldsymbol{n} = -\sum_{i=1}^{3} \mu_i \boldsymbol{n}_i$ to eliminate the variables x and y. We obtain

$$\mathcal{E}(\delta, \theta) \stackrel{\text{def}}{=} \sum_{i=1}^{3} \frac{\mu_i}{d_i l_i} \mathcal{C}_i(x, y, \theta, \delta) = \delta - A\cos(\theta - \alpha) - B, \tag{3}$$

where

$$A = \sqrt{C^2 + S^2}, \alpha = \text{Arg}(C, S), B = \textstyle\sum_{i=1}^{3} \frac{\mu_i}{l_i}(c_i + h_i),$$

$$C = \textstyle\sum_{i=1}^{3} \frac{\mu_i}{l_i}(a_i q_i + b_i r_i), S = \sum_{i=1}^{3} \frac{\mu_i}{l_i}(-b_i q_i + a_i r_i).$$

Note that the notation $\mathcal{E}(\theta, \delta)$ is justified by the fact that the value of $\mathcal{E}$ is independent of x and y. More

[1] Here, abusing the usual mathematical notation, $\text{Arg}(c, s)$ is the angle a such that $\cos(a) = c/\sqrt{c^2 + s^2}$ and $\sin(a) = s/\sqrt{c^2 + s^2}$.

importantly, it is now clear that a necessary condition for the existence of an object position achieving contact with the three pins is that the point (θ, δ) lies on the *contact sinusoid* defined by $\mathcal{E}(\delta, \theta) = 0$. This condition is also sufficient: for given values of θ and δ on this sinusoid, the three linear equations $\mathcal{C}_i(x, y, \theta, \delta)$ $(i = 1, 2, 3)$ in the two unknowns x and y are linearly dependent, and thus admit a common solution.

2.2 Equilibrium

At equilibrium, the various forces and moments exerted at the contacts balance each other. Exploiting the fact that the overall scale of the wrenches is irrelevant allows us to simply write the force equilibrium equation as $\boldsymbol{n} + \sum_{i=1}^{3} \mu_i \boldsymbol{n}_i = 0$. In turn, using (2) allows us to write the moment equilibrium equation as

$$\sum_{i=1}^{3} \lambda_i (\boldsymbol{v}_i \times \boldsymbol{n}) + \sum_{i=1}^{3} \mu_i [(\mathcal{R}^{-1}(\boldsymbol{q}_i - \boldsymbol{t})) \times \boldsymbol{n}_i] = 0, \quad \text{with} \quad \lambda_1 + \lambda_2 + \lambda_3 = 1 \quad \text{and} \quad \lambda_1, \lambda_2, \lambda_3 \geq 0. \tag{4}$$

Using again the relation $\boldsymbol{n} = -\sum_{i=1}^{3} \mu_i \boldsymbol{n}_i$ and writing the dot product of the contact moments and $\boldsymbol{n}$ in the (u, v, w) coordinate system yields

$$\sum_{i=1}^{3} \frac{\mu_i}{l_i} [(-b_i q_i + a_i r_i) \cos\theta - (a_i q_i + b_i r_i) \sin\theta] = 0,$$

or equivalently, $\sin(\theta - \alpha) = 0$.

It follows that a necessary condition for three pins in contact with the corresponding faces of the object to achieve equilibrium is that $\theta = \alpha$ or $\theta = \alpha + \pi$. Note that these values of θ are independent of the heights of the pins, which proves extremely important in grasp planning applications [12]. Equilibrium is necessary but not sufficient for immobility. Indeed, as shown in [12], the second-order condition for immobility of Rimon and Burdick [11] is only satisfied when $\theta = \alpha + \pi$.

2.3 Free Configuration Space Regions

Let us consider an immobilizing configuration of the gripper, defined by the position q_i, r_i and height h_i of the pins $(i = 1, 2, 3)$, by the position x_0, y_0 and orientation θ_0 of the object in the gripper's coordinate system, and by the jaw separation δ_0. We assume that the values of q_i, r_i and h_i are held constant and examine what happens when the separation of the jaws changes.

For a given jaw separation δ, the set $S_i(\delta)$ of object configurations (x, y, θ) for which $\mathcal{C}_i(x, y, \theta, \delta) = 0$ forms a ruled surface: indeed, its intersection with a plane $\theta =$ constant is a line $L_i(\delta, \theta)$ at distance $e_i - d_i\delta$ from the fixed point (q_i, r_i) of the x, y plane, and the angle between the x axis and the normal to this line is $\theta + \alpha_i$ (Figure 4). Changing θ corresponds to rotating the line about the point (q_i, r_i), while changing δ corresponds to translating the line.

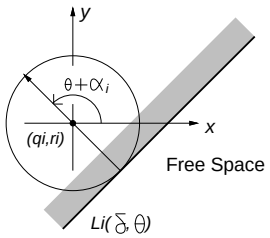

Figure 4. Contact between a pin and a face in configuration space.

The ruled surface $S_i(\delta)$ splits the three-dimensional space $\mathbb{R}^2 \times S^1$ of configurations x, y, θ into a "free" half-space $V_i(\delta)$ and a "forbidden" half-space $W_i(\delta)$ where pin number i penetrates the plane of f_i. Furthermore, $V_i(\delta)$ (resp. $W_i(\delta)$) is characterized by $\mathcal{C}_i(x, y, \theta, \delta) \geq 0$ (resp. ≤ 0).

Now let us consider the volume $V(\delta) = V_1(\delta) \cap V_2(\delta) \cap V_3(\delta)$. Given the form of $C_i(x, y, \theta, \delta)$, it is obvious that if a configuration lies in free space for some value δ_1 of δ, it also lies in free space for any other value $\delta_2 \geq \delta_1$. In other words, $V(\delta_1) \subset V(\delta_2)$ when $\delta_2 \geq \delta_1$ (this is also intuitively obvious since increasing δ corresponds to opening the jaws). In particular, the immobilizing configuration (x_0, y_0, θ_0) is always in free space for $\delta \geq \delta_0$.

The intersection of $V(\delta)$ with a plane $\theta =$ constant forms a triangular region $T(\delta, \theta)$. Note that the triangles corresponding to various values of θ are all homothetic since their edges make constant angles with each other. However, their size, position, and orientation varies with θ. Note also that these triangles, although possibly empty, are not degenerate: indeed, it is easy to verify that a necessary and sufficient for two edges of $T(\delta, \theta)$ to be parallel is that the normals to the corresponding faces be either equal or symmetric with respect to the vector $\boldsymbol{n}$, which contradicts the assumption that the directions $\boldsymbol{n}_i$ $(i = 1, 2, 3)$ and $\boldsymbol{n}$ positively span $\mathbb{R}^3$.

As shown in Figure 5, the region $T(\delta, \theta)$ may contain an open subset (Figure 5(a)), be reduced to a single point (Figure 5(b)), or be empty (Figure 5(c)).

In the second case (Figure 5(b)), the three pins simultaneously touch the corresponding faces, and $\mathcal{E}(\delta, \theta) = 0$. In fact, it is easy to show that a necessary and sufficient condition for $T(\delta, \theta)$ to contain at least one point is that $\mathcal{E}(\delta, \theta) \geq 0$: the condition is clearly

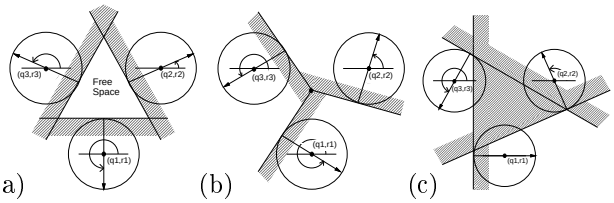

Figure 5. Possible configurations of the intersection $T(\delta,\theta)$ of $V(\delta)$ with a plane θ = constant: (a) $T(\delta,\theta)$ contains an open neighborhood; (b) it is reduced to an isolated point of the x,y plane; (c) it is empty.

necessary: since $\mathcal{E}(\delta,\theta)$ is by construction a convex combination of the functions $\mathcal{C}_i(x,y,\theta,\delta)$, the fact that $\mathcal{E}(\delta,\theta) < 0$ implies that, for any x,y, there exists some $i \in \{1,2,3\}$ such that $\mathcal{C}_i(x,y,\theta,\delta) < 0$. To show that the condition is also sufficient, let us assume that $T(\delta,\theta)$ is empty. This implies that, for any x,y, there exists some $i \in \{1,2,3\}$ such that $\mathcal{C}_i(x,y,\theta,\delta) < 0$. In particular, if (x_{12},y_{12}) is the point where the two lines associated with the faces f_1 and f_2 intersect (as remarked earlier, these lines are not parallel), we must have $\mathcal{E}(\delta,\theta) = (\mu_3/d_3l_3)C_3(x_{12},y_{12},\theta,\delta) < 0$.

This result allows us to characterize qualitatively the range of orientations θ for which $T(\delta,\theta)$ is not empty (Figure 6): for a given δ, the condition $\mathcal{E}(\delta,\theta) = 0$ is an equation in θ that may have zero, one, or two real solutions: a double root occurs at the minimum $\delta = \delta_0$ or at the maximum $\delta = \delta_{\max}$ of the sinusoid. In the former case, $\mathcal{E}$ is strictly positive everywhere except at $\theta = \alpha$ where it is equal to zero, and the range of orientations is S^1. In the latter case, the range of orientations reduces to a single point $\theta_0 = \alpha + \pi$. For any value δ_1 in the open interval $]\delta_0,\delta_{\max}[$, there are two distinct roots θ',θ'', and the range of orientations is the arc bounded by these roots and containing θ_0. Finally, for values of δ outside the $[\delta_0,\delta_{\max}]$ interval, there is no solution: either δ is strictly smaller than δ_0 and the range of orientations is empty (at least one of the pins penetrates the plane of the corresponding face), or δ is strictly larger than $\delta_{\max}$, and the range of orientations is S^1.

In particular, since the volume $V(\delta)$ is a stack of contiguous triangles $T(\delta,\theta)$, it is clear at this point that, for $\delta \geq \delta_0$, $V(\delta)$ is a non-empty, connected, compact region of $\mathbb{R}^2 \times S^1$. The analysis conducted in this section also gives some geometric insight on the immobility conditions derived in [12]. In particular, it confirms that the minimum point $(\alpha+\pi,\delta_0)$ of the contact sinusoid corresponds to an isolated point of configuration space or equivalently to an immobilizing configuration: indeed, the triangle $T(\delta_0,\alpha+\pi)$ is reduced to a point, and $T(\delta,\theta)$ is empty for any

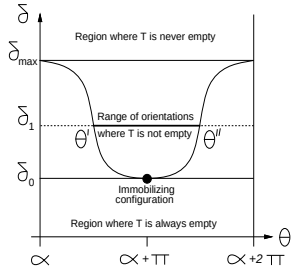

Figure 6. Regions of θ,δ space delimited by the sinusoid $\mathcal{E}(\delta,\theta) = 0$.

$\theta \neq \theta_0$. Likewise, although the maximum $(\alpha,\delta_{\max})$ of the sinusoid corresponds to an equilibrium grasp, it does not yield an immobilizing grasp since the object is free to undergo arbitrary rotations.

2.4 ICS Regions

The discussion so far has characterized the contacts between the pins and the planes of the corresponding faces, ignoring the fact that each face is in fact a convex polygon in its plane. Let us construct a parameterization of the set $E_i(\delta,\theta)$ of configurations (x,y) for which the tip of pin number i belongs to the corresponding face. Obviously, $E_i(\delta,\theta)$ is a subset of $L_i(\delta,\theta)$. This line is at distance $-d_i\delta + e_i$ from the point (q_i,r_i), with a normal whose orientation is $\theta+\alpha_i$; hence, it can be parameterized by

$$\begin{pmatrix} x-q_i \\ y-r_i \end{pmatrix} = (-d_i\delta+e_i)\begin{pmatrix} \cos(\theta+\alpha_i) \\ \sin(\theta+\alpha_i) \end{pmatrix} + \eta \begin{pmatrix} -\sin(\theta+\alpha_i) \\ \cos(\theta+\alpha_i) \end{pmatrix},$$

where η is some real parameter.

Using this parameterization and (2) yields

$$\begin{pmatrix} u_i \\ v_i \end{pmatrix} = (d_i\delta - e_i)\begin{pmatrix} \cos\alpha_i \\ \sin\alpha_i \end{pmatrix} - \eta \begin{pmatrix} -\sin\alpha_i \\ \cos\alpha_i \end{pmatrix}.$$

In turn, substituting these values in the inequalities (1) defining f_i yields a set of linear inequalities in η and δ. Actual contact occurs for pairs (η,δ) lying in the convex polygon defined by these constraints. It follows that for given values of δ and θ, $E_i(\delta,\theta)$ is a line segment, and the parameters η' and η'' associated with its endpoints are piecewise-linear functions of δ.

Now let us consider the three segments $E_i(\delta,\theta)$ $(i=1,2,3)$ together (Figure 7): if $E_i(\delta,\theta)$ and $E_j(\delta,\theta)$ intersect for all $i \neq j$, then the three segments completely enclose the triangle $T(\delta,\theta)$ (Figure 7(a)). We say that the corresponding configuration satisfies the *enclosure condition* since there is no escape path for the object in the x,y plane with the corresponding

orientation θ. More generally, when all triples of segments in the range of orientations associated with a given jaw separation δ satisfy the enclosure condition, $V(\delta)$ itself is an *inescapable configuration space* (ICS) region: in other words, the object is free to move within the region $V(\delta)$, but remains imprisoned by the grasp and cannot escape to infinity.

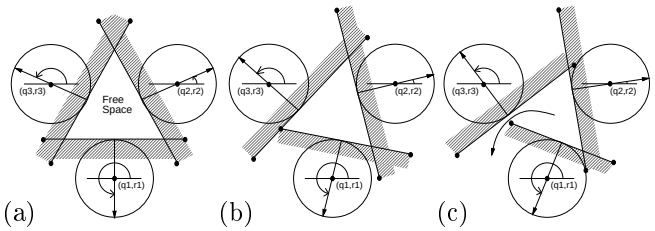

Figure 7. Triangle configurations: (a) three segments enclosing a triangle; (b) a critical configuration; (c) an opened triangle and an escape path.

2.5 Maximum ICS Regions

Here we address the problem of characterizing the maximum value δ^* for which $V(\delta)$ forms an ICS region for any δ in the $[\delta_0, \delta^*]$ interval. We know that at $\delta = \delta_0$ the three segments intersect at the immobilizing configuration, forming an ICS region reduced to a single point. Thus the enclosure condition holds at $\delta = \delta_0$. On the other hand, as $\delta \to +\infty$, the whole configuration space becomes free of obstacles, thus there must exist a critical point for some minimal value of δ greater than δ_0. This guarantees that δ^* has a finite value.

As shown by Figure 7(b), a critical event occurs when one of the endpoints of a segment lies on the line supporting another segment. After this event, the line segments fail to enclose the triangle $T(\delta, \theta)$ and the object can escape the grasp (Figure 7(c)).

According to the results established in the previous section, we can parameterize the coordinates of one of the endpoints of the segment $E_i(\delta, \theta)$ by $\eta = f_i\delta + g_i$ on the appropriate δ interval, with constants f_i and g_i determined by the coefficients a_{ij}, b_{ij} and c_{ij} of (1).

A critical event occurs when the endpoint under consideration is on the line $L_j(\delta, \theta)$ for some $j \neq i$. Substituting into $\mathcal{C}_i(x, y, \theta, \delta) = 0$ yields, after some simple algebraic manipulation

$$A_{ij}\cos(\theta + \beta_{ij}) + B_{ij}\delta + C_{ij} = 0, \qquad (5)$$

where

$$\begin{cases} A_{ij} = \sqrt{(q_i - q_j)^2 + (r_i - r_j)^2}, \\ \beta_{ij} = \alpha_j - \mathrm{Arg}(q_i - q_j, r_i - r_j), \\ B_{ij} = d_j - d_i\cos(\alpha_j - \alpha_i) + f_i\sin(\alpha_j - \alpha_i), \\ C_{ij} = -e_j + e_i\cos(\alpha_j - \alpha_i) + g_i\sin(\alpha_j - \alpha_i). \end{cases}$$

In other words, critical configurations form a second sinusoid in θ, δ space, called the *critical sinusoid* in the rest of this presentation.

We seek the minimum value of $\delta^* > \delta_0$ for which the range of orientations includes one of the critical orientations. As discussed above, we know that δ^* exists. Let us suppose first that a critical value lies in the interior of the range of orientations associated with some $\delta_1 \geq \delta_0$, and denote by $\delta_{\min}$ the minimum value of δ on the critical sinusoid. By definition, we have $\delta_1 \geq \delta_{\min}$. Suppose that $\delta_1 > \delta_{\min}$. Then by continuity, there exists some δ_2 such that $\delta_{\min} < \delta_2 < \delta_1$ and the corresponding range of orientations also contains a critical orientation (Figure 8). The argument holds for any value of $\delta > \delta_{\min}$. In other words, either the range of orientations of $\delta_{\min}$ contains a critical orientation, in which case $\delta^* = \delta_{\min}$ (Figure 8(a)), or it does not, in which case the critical value associated with δ^* must be one of its range's endpoints (Figure 8(b)). This is checked by intersecting the contact sinusoid and the critical one. Note that this process must be repeated six times (once per each segment/vertex pair) to select the minimum value of δ^*.

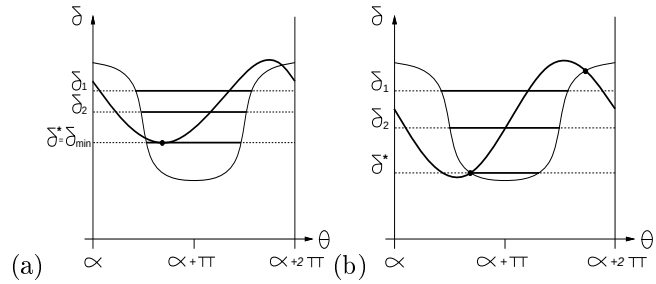

Figure 8. Critical configurations: (a) the critical configuration is the minimum of the critical sinusoid (shown as the thicker curve); (b) the critical configuration is the minimum intersection of the critical sinusoid and the contact sinusoid.

2.6 Main Result

The following lemma follows immediately from the results established in Sections 2.3, 2.4 and 2.5 and summarizes the findings of these sections.

Lemma 1: For given integer pin positions and heights q_i, r_i and h_i $(i = 1, 2, 3)$ and an immobilizing config-

uration $(x_0, y_0, \theta_0, \delta_0)$, there exists a critical jaw separation δ^* such that:
(1) for any $\delta > \delta^*$, there exists a path allowing the object to escape the grasp,
(2) for any δ in the interval $[\delta_0, \delta^*]$, the volume $V(\delta)$ is an inescapable region of configuration space that contains the configuration $(x_0, y_0, \theta_0, \delta_0)$,
(3) for any $\delta' \leq \delta''$ in the interval $[\delta_0, \delta^*]$, $V(\delta') \subset V(\delta'')$, and
(4) δ^* can be computed in closed form as the minimum of a sinusoid or the intersection of two sinusoids.

3 Algorithm

Lemma 2 can be used as a basis for in-hand manipulation by remarking that an object anywhere in the ICS region associated with some gripper configuration can be moved to the corresponding immobilized position and orientation by closing the gripper jaws (this follows immediately from properties (2) and (3) in Lemma 2). Thus we can plan manipulation sequences from one immobilized configuration to another by using the following algorithm:

Off-line:
(1) Compute the set S of all immobilizing configurations of the object.
(2) Construct a directed graph G whose vertices are the elements of S and whose edges are the pairs (s, s') of elements of S such that s belongs to the maximum ICS region ICS(s') associated with s'.
On-line:
(3) Given two configurations i and g in S, search the graph G for the shortest path going from the initial configuration i to the goal configuration g.

Once a path has been found, the corresponding manipulation sequence can be executed: starting from the configuration i, each edge (s, s') in the path allows us to move the object from s to s' by opening the jaws and retracting the pins associated with s, then lowering the pins associated with s' and closing the jaws.

3.1 Triples of Pins: Prototypes and Shifts

The grasp planning algorithm of [12] can be used to enumerate all immobilizing object/gripper configurations and implement Step (1). There is however a difference between grasping and manipulation applications: during grasp planning, one can always assume that the first pin is at the origin with zero height. Of course, when a grasp is actually executed, the pin positions and heights, along with the jaw separation, all have to be shifted so that the corresponding variables are all positive and the pin positions remain within the extent of the top plate. Nonetheless, gripper configurations that only differ by a shift of the three pin positions are equivalent for grasping purposes. This is not the case for in-hand manipulation, where the goal is to move the object held by the gripper across the bottom plate: this forces us to take into account all shifted configurations of a grasp.

We will say that a triple of pin positions with the first pin located at the origin is a *prototype*, and that all positions of the triple within the bottom plate are the *shifts* of this prototype. For each prototype, we can define the minimum rectangle aligned with the (p, q) coordinate axes and enclosing the pins. If W and H denote the width and height of this rectangle, and K^2 is the total number of grid elements, the prototype admits $(K-W)(K-H)$ different shifts, which can trivially be computed in time proportional to their number. As shown in [12], there are $O(D^2d^2)$ immobilizing prototypes, to which correspond $O(D^2d^4K^2)$ shifted object/gripper configurations. If we assume that the manipulated object fits completely on the gripper's bottom plate, note that we will have $d \leq D \leq K$.

3.2 Constructing the Graph

Constructing the graph G requires the ability to decide whether an immobilizing configuration s_a lies in the region ICS(s_b) associated with another configuration s_b. Let θ_a denote the orientation of the configuration s_a, and δ_b^* denote the critical jaw separation associated with s_b. A necessary condition for s_a to belong to ICS(s_b) is of course that s_a belongs to the range of orientations associated with δ_b^*.

When this necessary condition is fulfilled, let $T(\delta_b^*, \theta_a)$ denote the slice of ICS(s_b) at $\theta = \theta_a$. Then s_a will belong to ICS(s_b) if and only if s_a is inside $T(\delta_b^*, \theta_a)$. Note that constructing $T(\delta_b^*, \theta_a)$ does *not* require constructing an explicit boundary representation of ICS(s_b) then intersecting it with the plane $\theta = \theta_a$: instead, we construct the triangle directly from the lines $L_i(\delta_b^*, \theta_a)$ as explained in Section 2.3.

Thus constructing the graph only requires the ability of computing δ^* and the corresponding range or orientations, constructing the triangles $T(\delta^*, \theta)$ for discrete values of θ, and testing whether a point belongs to one of these triangles. Each one of these computations can be done in constant time.

From [12] and Section 2.2, we know that for a given triple of pins, all immobilizing configurations of

a given object will have the same orientation, independent of the pin heights. Of course, the immobilized orientation of the object remains the same when the triple of pins is arbitrarily shifted on the grid. Thus we can associate to each immobilizing prototype a plane θ =constant of the object's configuration space, and all the corresponding immobilizing configurations will lie in that plane. In other words, the vertices of the graph G will form layers of immobilized configurations corresponding to as many prototypes.

We now give an efficient algorithm for constructing the edges of the graph G. Let S_a and S_b be the sets of immobilized configurations corresponding to the layers $\theta = \theta_a$ and $\theta = \theta_b$ of the configuration space. We want to find all pairs of configurations s_a in S_a and s_b in S_b such that s_a lies within ICS(s_b) or equivalently within $T(\delta_b^*, \theta_a)$. This can of course be achieved by testing for each point-triangle pair whether the point belongs to the corresponding triangle. Instead, we observe that, following Section 2.3, the triangles $T(\delta_b^*, \theta_a)$ associated with all the elements of S_b are homothetic and, since θ is fixed, they also have the same orientation. This allows us to derive a more efficient method.

Let us restate the problem: given a set of points $P = \{p_1, p_2, .., p_n\}$, and a set $T = \{t_1, t_2, .., t_m\}$ of homothetic triangles having the same orientation, find all pairs (p_i, t_j) $(i = 1, .., n,\ j = 1, .., m)$ such that the point p_i is inside the triangle t_j (Figure 9). This type of query is common in computational geometry: for example, Chazelle gave an optimal $O(\log m + r)$ algorithm for the related problem of finding the subset of m isothetic rectangles which contain a query point, where r is the number of rectangles returned [3].

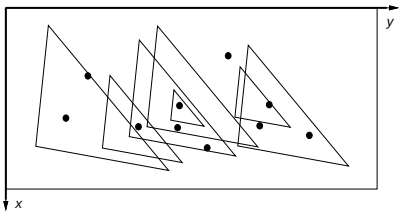

Figure 9. Points and triangles within the same layer.

This problem can be mapped onto another classical one through the following transformation: let $\boldsymbol{u}_i$ $(i = 1, 2, 3)$ denote the inward unit normals to the edges of the triangles. Given some choice of origin in the plane, we can associate with any point p its coordinates (x_1, x_2, x_3) along the vectors $\boldsymbol{u}_i$ (Figure 10). Likewise, we can associate with each triangle t the signed distances (y_1, y_2, y_3) between the origin and its edges along the vectors $\boldsymbol{u}_i$. Obviously p is inside t if and only if $x_i \geq y_i$ for $i = 1, 2, 3$. If we define the partial order $\succ$ over $\mathbb{R}^3$ by $(x_1, x_2, x_3) \succ (y_1, y_2, y_3)$ if and only if $x_i \geq y_i$ for $i = 1, 2, 3$, we have reduced our initial problem to the problem of finding the pairs of points p_i' in P' and t_j' in T' such that $p_i' \succ t_j'$, where P' and T' are subsets of $\mathbb{R}^3$ containing respectively n and m points. This is the problem called "3D Merge Dominance" by Preparata and Shamos [8, pp. 357–363], who give a simple divide-and-conquer algorithm for solving this problem in $O((m+n)\log(m+n) + s)$ time and $O(m+n)$ space, where s is the number of pairs found by the algorithm.

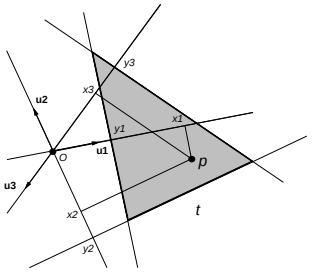

Figure 10. Three-dimensional coordinates associated with a point p and a triangle t.

3.3 Algorithm Analysis

The cost of the algorithm is dominated by the construction of the graph. Let V denote the number of immobilizing gripper configurations (or equivalently the number of vertices of G), and let P denote the number of prototypes associated with these configurations. Note that $P = O(D^2 d^2)$ and $V = O(P d^2 K^2)$ according to the analysis of [12]. Let E denote the number of edges of G. Since each prototype yields $O(d^2 K^2)$ shifted configurations and $d \leq K$, it follows from the analysis of the dominance algorithm that the construction of the graph takes $O(P^2 d^2 K^2 \log K + V + E)$ time. Of course, $E = O(V^2)$.

3.4 Implementation and Results

We have finished the mechanical assembly of the gripper, but are still in the final stages of completing the electronics and computer interface. Since our gripper is not operational yet, we can therefore only present simulated grasping experiments. We have implemented the manipulation planning algorithm, including its 3D dominance part, and tested our implementation using a 5×5 grid resolution. The program has been written in C, and all run times have been measured on a SUN SPARCstation 10.

Figure 11 shows an example of maximum ICS region in the configuration space (x, y, θ) for one of the

immobilized configurations of a tetrahedron. Note that this graphical representation is for display only: our algorithm does not construct an explicit boundary representation of the ICS. Instead, we compute the corresponding δ^* value and the associated range of orientations. Our grasp planning program finds 208 prototypes and 33,868 shifted immobilizing configurations, and the corresponding ICS computation takes 13 seconds. The graph G contains 1,247,374 edges, and its construction takes 156 seconds. Once the graph has been constructed, the search for sequences of gripper configurations is quite efficient: a simple breadth-first approach has been used in our experiments to search the graph G, and the search time is below 1 second in all cases.

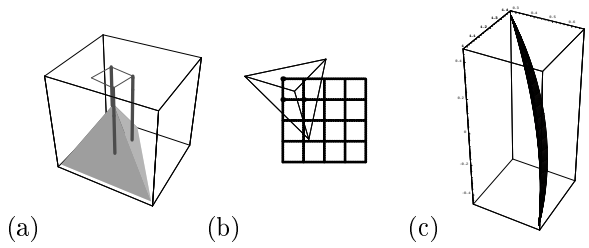

Figure 11. An ICS region in configuration space: (a)-(b) two views of an immobilized configuration of a tetrahedron; (c) the corresponding ICS region.

Figure 12 shows two examples. In the first one, the program finds a 4-step sequence to move the object from the configuration shown in Figure 12(a) to the one shown in Figure 12(b). Note that, although the pin configurations are the same in Figures 12(c) and 12(d), the pin lengths are actually different, yielding different object positions. Figure 12(e)-(g) shows a more complicated example, where the program finds a 72-step sequence of gripper configurations (Figure 12(g)) to move the object from the configuration shown in Figure 12(e) to the one shown in Figure 12(f).

Acknowledgments: This research was supported in part by the National Science Foundation under grant IRI-9634393, by a Critical Research Initiative planning grant from the University of Illinois at Urbana-Champaign, and by an equipment grant from the Beckman Institute for Advanced Science and Technology.

References

[1] S. Akella and M.T. Mason. Parts orienting by push-aligning. In *IEEE Int. Conf. on Robotics and Automation*, pages 414–420, Nagoya, Japan, May 1995.

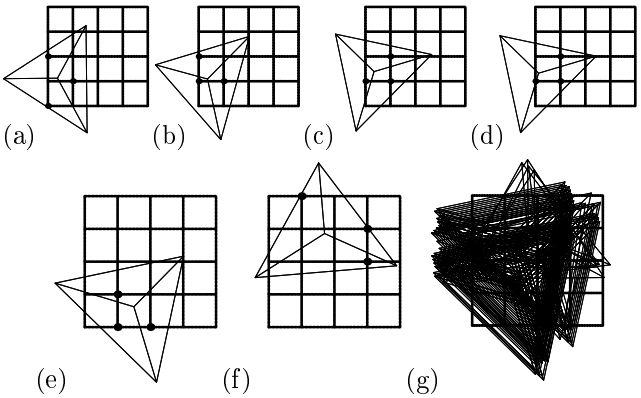

Figure 12. Two examples of manipulation sequences. See text for details.

[2] J.F. Canny and K.Y. Goldberg. "RISC" for industrial robotics: recent results and open problems. In *IEEE Int. Conf. on Robotics and Automation*, pages 1951–1958, San Diego, CA, 1994.

[3] B.M. Chazelle. Filtering search: a new approach to query answering. In *IEEE Symposium on Foundations of Computer Science*, pages 122–132, Tucson, AZ, November 1983.

[4] M.A. Erdmann and M.T. Mason. An exploration of sensorless manipulation. *IEEE Journal of Robotics and Automation*, 4:369–379, 1988.

[5] K.Y. Goldberg. Orienting polygonal parts without sensors. *Algorithmica*, 10(2):201–225, 1993.

[6] K.M. Lynch and M.T. Mason. Stable pushing: mechanics, controllability, and planning. In K.Y. Goldberg, D. Halperin, J.-C. Latombe, and R. Wilson, editors, *Algorithmic Foundations of Robotics*, pages 239–262. A.K. Peters, 1995.

[7] M.T. Mason. Mechanics and planning of manipulator pushing operations. *International Journal of Robotics Research*, 5(3):53–71, 1986.

[8] F.P. Preparata and M.I. Shamos. *Computational Geometry - An Introduction*. Springer-Verlag, 1985.

[9] A.S. Rao and K.Y. Goldberg. Manipulating algebraic parts in the plane. *IEEE Transactions on Robotics and Automation*, pages 598–602, 1995.

[10] E. Rimon and A. Blake. Caging 2D bodies by one-parameter two-fingered gripping systems. In *IEEE Int. Conf. on Robotics and Automation*, pages 1458–1464, Minneapolis, MN, April 1996.

[11] E. Rimon and J. W. Burdick. Towards planning with force constraints: On the mobility of bodies in contact. In *Proc. IEEE Int. Conf. on Robotics and Automation*, pages 994–1000, Atlanta, GA, May 1993.

[12] A. Sudsang, N. Srinivasa, and J. Ponce. On planning immobilizing grasps for a reconfigurable gripper. In *IEEE/RSJ International Conference on Intelligent Robots and Systems*, 1997. Accepted for publication.

[13] A. Wallack and J.F. Canny. Planning for modular and hybrid fixtures. In *IEEE Int. Conf. on Robotics and Automation*, pages 520–527, San Diego, CA, 1994.

[14] A.S. Wallack. *Algorithms and Techniques for Manufacturing*. PhD thesis, Computer Science Division, Univ. of California at Berkeley, 1995.